ACS OMEGA

http://pubs.acs.org/journal/acsodf

Article

Prediction for Plasma Trough Concentration and Optimal Dosing of Imatinib under Multiple Clinical Situations Using Physiologically Based Pharmacokinetic Modeling

Dongmei Gao, Guopeng Wang,[#] Honghai Wu, JinHua Wu,* and Xiaoang Zhao*

Cite This: *ACS Omega* 2023, 8, 13741−13753

Read Online

ACCESS | Metrics & More | Article Recommendations | Supporting Information

ABSTRACT: (1) *Purpose*: This study aimed to develop a physiologically based pharmacokinetic (PBPK) model to predict the trough concentration (C_{trough}) of imatinib (IMA) at steady state in patients and to explore the role of free concentration (f_{up}), α1-acid glycoprotein (AGP) level, and organic cation transporter 1 (OCT1) activity/expression in clinical efficacy. (2) *Methods*: The population PBPK model was built using physicochemical and biochemical properties, metabolizing and transporting kinetics, tissue distribution, and human physiological parameters. (3) *Results*: The PBPK model successfully predicted the C_{trough} of IMA administered alone in chronic phase (CP) and accelerated phase (AP) patients, the C_{trough} of IMA co-administered with six modulators, and C_{trough} in CP patients with hepatic impairment. Most of the ratios between predicted and observed data are within 0.70−1.30. Additionally, the recommendations for dosing adjustments for IMA have been given under multiple clinical uses. The sensitivity analysis showed that exploring the f_{up} and AGP level had a significant influence on the plasma C_{trough} of IMA. Meanwhile, the simulations also revealed that OCT1 activity and expression had a significant impact on the intracellular C_{trough} of IMA. (4) *Conclusion*: The current PBPK model can accurately predict the IMA C_{trough} and provide appropriate dosing adjustment recommendations in a variety of clinical situations.

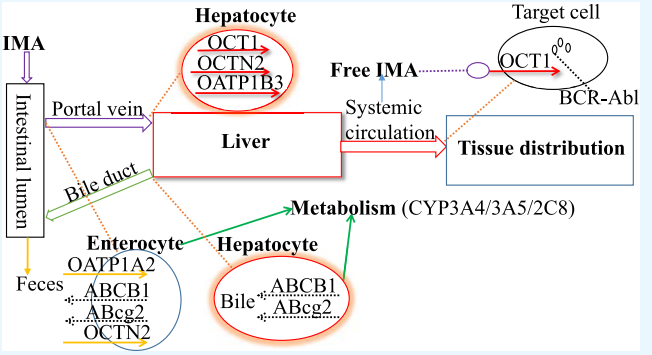

1. INTRODUCTION

Imatinib (IMA) is the first selective tyrosine kinase inhibitor that primarily targets BCR-Abl. It is clinically indicated for the treatment of patients with Philadelphia chromosome-positive chronic myeloid leukemia (Ph + CML) approved in 2001 and gastrointestinal stromal tumor (GIST) approved in 2002 by the FDA in blast crisis (BC), accelerated phase (AP), or chronic phase (CP).[1,2] Dosage strengths were approved as 100 mg and 400 mg tablets for oral administration of 300−600 mg once daily (OD) for patients.[2]

CYP2C8 (cytochrome P450) and CYP3A4 are the major enzymes responsible for the biotransformation of *N*-desmethyl IMA.[3] CYP3A5, CYP2D6, and CYP2C9 enzymes play a minor role in the formation of the *N*-desmethyl IMA.[3,4] It was reported that at least 14 metabolites were present in human plasma, urine, and feces.[5] Of these metabolites, only the metabolite *N*-desmethyl IMA exhibits inhibitory activity towards BCR-Abl similar to IMA.[6] However, the plasma AUC of *N*-desmethyl IMA is about 13.1% of the area under curve (AUC) for IMA.[5] Moreover, the *in vivo* distribution of IMA is involved in multiple transporters. IMA is a substrate for the influx organic cation transporter 1 (OCT1).[7] Likewise, *in vitro* data indicated that IMA was also a substrate for efflux transporters *p*-glycoprotein (*p*-gp)[8] and organic anion transporting polypeptides 1B1 (OATP1B1)[9] and influx ATP binding cassette subfamily G member 2 (Abcg2)[10] as well as an inhibitor of human *p*-gp with a K_i of 18.3 μM.[8] Of these transporters, OCT1 is the only influx transporter for which it has been clinically reported that a higher dose, even up to 800 mg/day, was needed to overcome the negative impact of low activity and expression in CML patients.[11]

The research on exposure−response relationships in patients has suggested that clinical efficacy is strongly correlated with the trough concentration (C_{trough}) of IMA at steady state. A large number of studies have suggested a minimum concentration (i.e., C_{trough}) of ≥1000 ng/mL as a pharmacokinetics (PK) threshold for optimal clinical efficacy.[12−14] In addition, clinical analyses between exposure and side events have found that the frequency of neutropenia in patients with CML-CP can reach 37% within 12 months when the C_{trough} is above 3180 ng/mL.[15] However, the converted maximum

Received: December 14, 2022
Accepted: March 23, 2023
Published: April 3, 2023

human dose is 800 mg/day based on the body surface area according to teratogenic toxicity in rats.[16,17] The reported mean C_{trough} of IMA at 800 mg is 2690 ng/mL in CML patients[15] and 3330 ng/mL in GIST patients[18] in the clinical research. As a result, a PK threshold of 1000 ng/mL ≤ C_{trough} ≤ 3010 ng/mL (mean of 2690 and 3330 ng/mL) is appropriate for clinical efficacy and safety.

Multiple factors can influence the human C_{trough} of IMA, including different disease statuses (CP and AP), co-administration with CYP3A4 modulators (drug−drug interaction, DDI), insufficient hepatic function, and CYP3A4/CYP2C8 genetic polymorphisms. The previous studies have demonstrated that the AUC of IMA was increased by 40% with ketoconazole[19] (a strong CYP3A4 inhibitor) co-administration and decreased by 68% upon concomitant use with rifampicin[20] (a strong CYP3A4 inducer). Additionally, the clinical study has displayed that the dose of IMA should be increased to 600 even to 800 mg/day to achieve a better clinical response because of the low activity and expression of OCT1.[11]

Despite high solubility, permeability (BCS I),[21] and oral bioavailability of IMA,[2] the huge interpatient variations, even a 54[22] and 58%[23] coefficient of variation (CV), were still observed in the multiple papers. The IMA C_{trough} is strongly correlated with clinical response. A large C_{trough} variation can lead to ineffective clinical therapy. According to the observations in the clinic,[3,11] the difference in expression and activity of metabolizing enzyme and OCT1 between different patients can be two main influencing factors. In addition, IMA highly binds to α1-acid glycoprotein (AGP), with plasma protein binding of 92−95% in healthy humans and patients with different disease statuses (AP and CP).[24] Also of note is that it has been evidence that the AGP level in patients with CML is significantly higher compared with healthy humans[6] and that patients in AP have a significantly higher AGP level than those in CP.[25] It has been observed that an increased AGP level can significantly reduce systemic exposure of IMA.[6] As a result, the difference of f_{up} (plasma free IMA concentration) and AGP level between different patients may be important factors influencing C_{trough} variation. Additionally, different administered doses were proposed for patients at different disease statuses in CP (400 mg/day) and AP (600 mg/day). What is the primary cause of the difference in C_{trough} levels between patients at various stages? The large difference in f_{up}, AGP level, and OCT1 activity and expression in healthy humans and patients at different phases can be the main cause.

Currently, four papers are involved in the physiologically based pharmacokinetic (PBPK) model of IMA.[26−29] Nevertheless, only two of them have great applied value.[28,29] The work by Adiwidjaja et al. primarily focused on the applications of PK in pediatrics using the PBPK model[28] and the predictions of interethnic differences in PK of IMA.[29] When taking IMA in patients in various clinical situations (such as those in AP or CP, DDI caused by CYP3A4/2C8 and OCT1 and patients with hepatic impairment), the IMA C_{trough} threshold should be considered as a key factor in determining the optimum dosing regimens. Therefore, we developed a PBPK model in healthy humans and patients in CP and AP and used it to (i) predict the C_{trough} of IMA in patients in CP and AP, respectively, (ii) predict C_{trough} alterations of IMA upon concomitant use with CYP3A4/2C8/OCT1 modulators and in patients with liver dysfunction, (iii) analyze the effect of f_{up}, AGP level and OCT1 activity/expression on IMA C_{trough} by the sensitivity analysis, and (iv) recommend an appropriate dosing regimen in the patients under various clinical situations based on the C_{trough} threshold for the efficacy and safety.

2. MATERIALS AND METHODS

2.1. Software. The PK-Sim (Version 10.0, Bayer Technology Services, Leverkusen, Germany) was used to build the PBPK model; Digit (Version 1.0.4, Simulations Plus) was used to digitize the figures of PK profiles of IMA from published papers. Origin 2019 (version 9.6.5.169, OriginLab) was used to draw the figures.

2.2. PBPK Model Development and Verification. *2.2.1. PBPK Model Development.* In the PBPK model, the human tissue distribution and cellular permeability of IMA were described by Rodgers and Rowland and PK-Sim standard methods, respectively. The biotransformation of IMA to *N*-desmethyl IMA was described by Michaelis−Menten kinetics, and K_m and V_{max} were assigned as 1.4 μM and 0.41 pmol/min/pmol for CYP2C8[3] and as 10.5 μM for CYP3A4,[28] respectively. The CYP3A4 V_{max} was optimized to 6.0 pmol/min/pmol to better fit the observed PK profiles. The metabolism of IMA to other metabolites was described by intrinsic clearance (CL_{int}). The $CL_{int,u}$ values for CYP2C8 and CYP3A4 were 24.2 and 33.4 μL/min/mg protein, respectively.[28] The active uptake of IMA via OCT1 into cells was also depicted by Michaelis−Menten kinetics. The V_{max} value for OCT1 in healthy humans was calculated as 128.1 pmol/min/pmol by V_{max} (50.5 nmol/mg protein/10 min) in the paper[7] × protein expression (37.3 mg/g liver tissue)[30] × liver weight (1855.8 g for a 74.2 kg person)[31] × concentration (0.077 μM/L liver tissue)[32] × liver volume (mean 2.38L, built-in PK-Sim). Based on published studies,[7] V_{max} for OTC in diseased cells is about 40% of that in healthy status. As a result, the V_{max} values for OCT1 in CP and AP patients were calculated as 50.7 pmol/min/pmol. The V_{max} values of OATP1A2, OATP1B3, and OCCN2 were calculated to be 72.5, 57.7, and 67.6 pmol/min/g tissue by ratio of the cumulative transported amount and those by OCT1 (about 0.5 pmol/min/million cells).[9] The V_{max} values for ABCB1 and ABcg2 were converted based on the relationship of g tissue equivalent to 120 million cells.[28] The K_m values for OATP1A2, OATP1B3, OCTN2, and ABCB1 were optimized using the parameter identification module of PK-Sim.

The PBPK model of IMA contains three metabolizing enzymes (CYP2C8 and CYP3A4/3A5) and six influx/efflux transporters (OCT1, OATP1A2, OATP1B3, OTCN2, ABCB1, and ABcg2). Except for the three metabolizing enzymes, the reference concentrations of six transporters were not built into the PK-Sim expression database. The OCT1 expression was obtained from the paper.[32] For OATP1A2,[33] OATP1B3,[34] OTCN2,[35] ABCB1,[35] and ABcg2,[35] the reference concentration was calculated using the formula (transporter protein abundance × expressed organ weight)/liver volume.

The f_{up} values for healthy humans, CP patients, and AP patients were assigned as 0.074,[24] 0.05, and 0.05 (mean value of AML patients),[6,24] respectively. Also, the mean AGP level in healthy humans and CP and AP patients was determined to be 0.62, 0.92, and 1.32, respectively.[25] In the PBPK model, the CV% of every population in AGP concentration was set at 15%. The change in AGP level between different populations was described using the plasma protein scale factor (PPSF) in the PK-SIM. PPSF was estimated by.[32]

https://doi.org/10.1021/acsomega.2c07967
ACS Omega 2023, 8, 13741−13753

Table 1. Summary of Parameters Used in the PBPK Model

property (units)		values used in the model	literature values and source	descriptions
MW (g/mol)		493.61	chemspider	molecular weight
pK_a (dibasic base)		3.9, 7.7	3.9, 7.7[37]	base dissociation constant
log P		1.1	−2.0 (pH 1.0) to 2.0 (pH 6.8)[36]	lipophilicity
solubility (mg/mL)		0.1 (pH 6.0)	0.1 (pH 6.0)[36]	
P_{app} ($\times 10^{-6}$ cm/s)		0.95	0.95[4]	Caco-2 cell permeability
f_{up}		0.074,[a] 0.05,[b] 0.04[c]	7.4 and 5.0%[24]	fraction of free drug in plasma
Rbp		1.6	optimized	blood-to-plasma concentration ratio
CYP3A4 V_{max} (pmol/min/pmol)		6.0	3.0[28]	maximum metabolism velocity for converting to *N*-desmethyl IMA
CYP2C8 V_{max} (pmol/min/pmol)		0.41	0.41, 44.1[3]	
CYP3A5 V_{max} (pmol/min/pmol)		44.1		
CYP3A4 K_m (μM)		10.5	10.5[28]	Michaelis−Menten constant for converting to *N*-desmethyl IMA
CYP2C8 K_m (μM)		1.4	1.4, 43[3]	
CYP3A5 K_m (μM)		43		
CYP3A4 $CL_{int,u}$ (μL/min/mg protein)		24.2	24.2, 33.4[28]	intrinsic clearance for the other metabolites
CYP2C8 $CL_{int,u}$ (μL/min/mg protein)		33.4		
OCT1 V_{max} (pmol/min/pmol)		128.1,[a] 50.7[b,c]	50.5 nmol/10 min/mg protein	maximum efflux/influx velocity for OCT1, OATP1B1, OATP1B3, OCTN2, ABCB1, and ABcg2
V_{max} (pmol/min/ g tissue)	OATP1A2	72.5	calculated	
	OATP1B3	57.7		
	OCTN2	67.6		
	ABCB1	12.5	1.5, 89.4 pmol/min /million cells	
	ABcg2	0.75		
OCT1 K_m (μM)		36.2	26.2[7]	Michaelis−Menten constant for OCT1, OATP1B1, OATP1B3, OCTN2, ABCB1, and ABcg2
OATP1A2		63.2	optimized	
OATP1B3		80.3		
OCTN2		76.3		
ABCB1		20.3		
ABcg2		4.37	4.37[28]	
CL_R (L/h)		GFR × f_{up}	GFR × f_{up}	renal clearance
GFR fraction		1.0		fraction of filtered drug in the urine
PPSF		1.0,[a] 1.45,[b] 2.02[c]	calculated using formula 1	plasma protein scale factor
K_p scale		5.0	optimized	organ-to-plasma partition coefficient
partition coefficients		Rodgers and Rowland	optimized	calculation method from cell to plasma coefficients
cellular permeabilities		PK-Sim Standard	optimized	permeability calculation method across cell
reference concentration (μM/L liver tissue)	CYP3A4	4.32	default	reference concentration for metabolizing enzyme and transporters
	CYP2C8	2.56		
	CYP3A5	0.04		
	OCT1	0.077	0.077[32]	
	OATP1A2	1.31	calculated	
	OATP1B3	0.30		
	OCTN2	0.0027		
	ABCB1	0.68		
	ABcg2	0.13		
K_i CYP3A4 (μM)		14.3	14.3[39]	inhibition constant at CYP3A4
K_{inact} CYP3A4 (min^{-1})		0.072	0.072[39]	the maximum rate of inactivation against CYP3A

[a]For healthy humans. [b]For CP patients. [c]For AP patients.

$$\mathrm{PPSF} = \frac{1}{f_{up} + (1 - f_{up}) \times \mathrm{AGP_f}} \quad (1)$$

where AGP_f is the fractional value of the compared AGP level in healthy humans compared with AGP in CP and AP patients. The renal clearance (CL_R) was estimated by the glomerular filtration rate (GFR) × f_{up} method in PK-Sim. The log P of IMA spans from −2.0 (pH 1.0) to 2.0 (pH 6.8);[36] in this simulation, the log P was set at 1.1. In this model, the effect of kidney transporters or tubules on the uptake or excretion of IMA was not considered, and as a result, the fraction of GFR was set at 1.0. K_p scale was optimized to 5.0 to better describe the tissue distribution of IMA.

The demographic characteristics data used in the PBPK model were taken from each corresponding clinical study, and the virtual population information includes age range, body weight, height, and proportion of female participants. If some data was unavailable, the mean value built-in PK-Sim was used as a surrogate. The final parameters of the model are summarized in Table 1.[37−39]

https://doi.org/10.1021/acsomega.2c07967
ACS Omega 2023, 8, 13741−13753

Table 2. Comparisons of the Arithmetic Mean C_{trough} between Predicted and Observed Data in CP and AP Patients[a]

			C_{trough} (ng/mL) ± SD		$AUC_{(0-24)}$ (μg·h/mL) ± SD		C_{max} (ng/mL) ± SD		prediction/observation ratio		
clinical study	disease and phase	dose (mg/day)	prediction	observation	prediction	observation	prediction	observation	C_{trough}	AUC	C_{max}
Peng et al.[42]	CML, CP	25	38 ± 14	41 ± 21	1.85 ± 0.43	1.9 ± 0.9	130.3 ± 24.3	179.9 ± 89.2	0.93	0.97	0.72
		50	87 ± 29	109 ± 14	3.97 ± 0.95	4.6 ± 0.4	272.4 ± 61.3	365.7 ± 75.6	0.80	0.86	0.74
		140	315 ± 124	279 ± 38	13.0 ± 3.2	12.1 ± 1.4	839.9 ± 168.0	1053.8 ± 236.3	1.13	1.07	0.80
		300	860 ± 452	886 ± 752	31.7 ± 8.2	27.4 ± 11.5	1961.4 ± 413.7	1834.2 ± 668.4	0.97	1.16	1.07
		400	1228 ± 720	1216 ± 750	44.4 ± 11.7	40.1 ± 15.7	2702.0 ± 820.3	2596.0 ± 786.7	1.01	1.11	1.04
		600	2136 ± 764	1214 ± 817	71.3 ± 19.0	51.7 ± 26.7	4248.2 ± 931.5	3508.9 ± 1649.3	1.76	1.38	1.21
		750	2899 ± 1118	1447 ± 582	92.6 ± 24.6	56.4 ± 20.2	5456.2 ± 1200	3804.8 ± 1488.7	2.00	1.64	1.43
Forrest et al.[13]	CML, CP	400	1268 ± 552	1175 ± 656	--	-	--	-	1.08		
	CML, AP	600	1243 ± 726	1067 ± 473	--	-	--	-	1.16		
Yoo et al.[18]	GIST, CP	300	984 ± 454	1305 ± 633	--	-	--	-	0.75		
		400	1358 ± 663	1452 ± 830	--	-	--	-	0.94		
		600	2017 ± 850	1698 ± 725	--	-	--	-	1.19		
		800	3170 ± 1320	3330 ± 1592	--	-	--	-	0.95		
Guilhot et al.[15]	CML, CP	300	963 ± 382	1040 ± 864	--	-	--	-	0.93		
		400	1238 ± 517	1200 ± 931	--	-	--	-	1.03		
		600	2033 ± 948	1935 ± 756	--	-	--	-	1.05		
		800	3233 ± 1040	2690 ± 1231	--	-	--	-	1.20		
Farag et al.[22]	GIST, CP	400	1331 ± 795	1231 ± 934	--	-	--	-	1.08		
Ogata et al.[43]	CML, CP	300	895 ± 328	934 ± 117	--	-	--	-	0.96		
		400	1297 ± 777	1429 ± 451	--	-	--	-	0.91		
IJzerman et al.[44]	GIST, CP	400	1196 ± 507	1074(946−1247)	--	-	--	-	1.11		

[a]SD: standard error; -: not reported clinical data; --: not calculated data; empty: no data.

https://doi.org/10.1021/acsomega.2c07967
ACS Omega 2023, 8, 13741−13753

2.2.2. PBPK Model Verification. Multiple clinically observed PK profiles of IMA in healthy subjects[40,41] and in CP patients with CML[42] were employed to validate the predictive accuracy of the PBPK model. The prediction accuracy of the PBPK model was evaluated using the ratio between predicted and observed PK parameters (AUC, C_{max} and C_{end}). Subsequently, the PBPK model was further verified by comparing the predicted and observed C_{trough} in AP and CP patients[13,15,18,22,42−44] at eight doses for consecutive 15 days. Generally, the commonly acceptable criterion is within 0.5−2.0; however, in our study, the acceptable criterion was set within 0.7−1.3.

2.3. Sensitivity Analysis. The sensitivity analysis was carried out to determine the effect of the selected model parameters on the C_{trough} for CP and AP patients. The standard dose regimens were given at 400 mg OD in CP patients and 600 mg OD in AP patients, respectively, for consecutive 14 days. The modeling parameters were selected in the sensitivity analysis according to the following criteria: (1) optimized and (2) could have a strong impact on the C_{trough} in this model. The selected parameters were (i) log *P*, (ii) f_{up}, (iii) Rbp, (iv) PPSF, (v) CYP3A4/2C8 V_{max} and OCT1 V_{max}, (vi) K_M and V_{max} for OATP1A2, OATP1B3, OCTN2, and ABCB1, (vii) expression (CYP3A4/2C8, OCT1), (viii) liver volume, and (ix) K_i CYP3A4.

The effects of the selected parameters on the C_{trough} were evaluated by altering the value of each parameter by ± 20%.[45] The sensitivity coefficient (SC) is calculated as follows[45]

$$SC = \Delta Y/Y \div \Delta P/P \quad (2)$$

where ΔY is the alteration of predicted C_{trough}; Y is the initial value of predicted C_{trough}; ΔP is the alteration of model parameters; and P is the initial value of assessed parameters. If a certain SC absolute value is above 1.0 (i.e., it means that a 20% change of the assessed parameters results in a 20% alteration in C_{trough}), it means that this model parameter has a significant influence on predicted C_{trough}.

2.4. Applications of the PBPK Model. *2.4.1. C_{trough} Prediction in CP and AP Patients.* In the PBPK population simulations, both the disease and phase of patients and dosage were set according to the clinical papers (Table 2). The IMA was administered for consecutive 14 days. It was assumed that steady state could be reached after 14 days of taking IMA.

2.4.2. C_{trough} Prediction under DDI. The developed PBPK model of IMA was combined with the PBPK models of CYP3A4 inhibitors (ketoconazole and itraconazole) and inducers (rifampicin and efavirenz), CYP2C8 inhibitors (montelukast) and inducers (rifampicin), and OCT1 inhibitors (verapamil), respectively, to predict IMA C_{trough} changes under DDI. The inhibition and induction parameters of modulators are listed in Table 3.[46−51]

During DDI simulations, the IMA dosage regimens were designed as multiple doses for CP patients. The dosage regimens of the inhibitors and inducers are given in Table 4. The virtual demographic characteristics data in the DDI simulations with ketoconazole and rifampicin were taken from the published papers.[19,20] However, because of the unavailability of clinical DDI data, the virtual demographic characteristics data of the other DDI simulations are performed using the same demographic characteristics as the simulations with ketoconazole in this study.

The DDI simulation was first validated using the clinically observed PK profiles of IMA (200 mg OD for consecutive 7 days) when administered with ketoconazole.[19] Following that, the C_{trough} values of IMA were predicted under multiple DDI scenarios. The final modeling parameters used in the PBPK models for all of the modulators are listed in Supporting Table S1.

Table 3. Inhibition and Induction Parameters of Modulators

modulators	K_i (μM)	EC_{max}	EC_{50} (μM)
Ketoconazole[46]	0.015 (CYP3A4)		
Itraconazole[47]	0.0013 (CYP3A4)		
Hydroxy-itraconazole[47a]	0.0023 (CYP3A4)		
Rifampicin[48,49]		9.0 (CYP3A4)	0.34
		10.0 (CYP2C8)	0.12
Efavirenz[b]		5.2 (CYP3A4)	0.07
Montelukast[50]	0.02 (CYP2C8)		
Verapamil[51]	2.0 (OCT1)		

[a]Metabolite of itraconazole. [b]Built-in PK-Sim.

2.4.3. C_{trough} Prediction in Patients with Hepatic Impairment. The physiological parameters used in patients with hepatic dysfunction were obtained from the published papers and are summarized in Supporting Table S2. The IMA dosage regimens were set for CP patients with wild (at 300, 400, 500, and 600 mg OD), moderate (at 200, 300, and 400 mg OD), and severe (at 100, 200, and 300 mg OD) hepatic impairments. The virtual demographic characteristics data in this simulation correspond to those in the paper.[52,53] The simulations in CP patients with hepatic impairment were validated by comparisons with the clinically observed PK data.[52,53] Next, the C_{trough} values in CP patients with mild, moderate, and severe hepatic impairment were predicted by the PBPK model, respectively, after IMA was administered under multiple dosages for consecutive 14 days (see Table 4).

3. RESULTS

3.1. Validation of the PBPK Model. Figure 1 shows the generic workflow of the PBPK model for IMA. The population PBPK model was built based on the modeling parameters, absorption, metabolism, and distribution processes involved in multiple metabolizing enzymes and transporters. The model was validated using multiple PK profiles in healthy humans and CP patients, using ratios between predicted and observed C_{trough}, using PK profiles in healthy humans when co-administered with ketoconazole, and using PK profiles in CP patients with hepatic impairment. Subsequently, the PBPK model displayed a wide application in four aspects. Finally, the PBPK model was used to determine the optimal dosing regimens in various clinical settings.

The predicted and observed plasma concentration−time profiles in healthy subjects are shown in Figure 2A (an infusion of 100 mg IMA in 60 min) and 2B (single oral administration of 400 mg IMA). Figure 2C−F shows the predicted and observed plasma concentration−time profiles in CP patients. As seen in Figure 2, the population PBPK model may reproduce the clinically determined PK profiles.[40−42] The predicted and observed arithmetic mean PK parameters are shown in Figure S1. All three predicted/observed ratios (AUC, C_{max}, and C_{end}) were in the range of 0.7−1.3 (Figure S1). The goodness-of-fit plot (Figure S1) visually demonstrates a good fit of the PBPK model of IMA.

https://doi.org/10.1021/acsomega.2c07967
ACS Omega 2023, 8, 13741−13753

Table 4. IMA Dosing Adjustment Recommendations Based on the PBPK Model

scenarios		arithmetic mean C_{trough} (ng/mL) ± SD	based-model recommendation
DDI (IMA + ketoconazole 400 mg OD)			
300 mg OD		1075 ± 395	no need to adjust dose
400 mg OD		1519 ± 575	
DDI (IMA + itraconazole 200 mg BID)			
200 mg OD		1040 ± 450	support dose reduction to 300 mg OD
300 mg OD		1556 ± 767	
400 mg OD		2103 ± 958	
DDI (IMA + rifampicin 600 mg OD)			
400 mg OD		193 ± 86	avoid concomitant use or adjust dose to 400 mg BID
800 mg OD		744 ± 364	
400 mg BID		1304 ± 417	
DDI (IMA + efavirenz 600 mg OD)			
400 mg OD		484 ± 285	avoid concomitant use or adjust dose to 800 mg OD or 300 mg BID
600 mg OD		987 ± 440	
800 mg OD		1585 ± 633	
200 mg BID		767 ± 343	
300 mg BID		1442 ± 683	
DDI (IMA + montelukast 10 mg OD)			
400 mg OD		1170 ± 491	no need to adjust dose
DDI (IMA + verapamil 80 mg BID)			
300 mg OD		1020 ± 486	no need to adjust dose
400 mg OD		1446 ± 623	
hepatic impairment			
mild	300 mg OD	880 ± 354	no need to adjust dose
	400 mg OD	1275 ± 511	
	500 mg OD	1703 ± 626	
moderate	200 mg OD	603 ± 205	
	300 mg OD	1017 ± 466	
	400 mg OD	1474 ± 512	
severe	200 mg OD	748 ± 367	support dose adjustment to 300 mg OD
	300 mg OD	1196 ± 388	
	400 mg OD	1665 ± 729	

3.2. Sensitivity Analysis. As shown in Figure 3, the ten sensitive parameters to the IMA C_{trough} are represented. The most sensitive parameters in both CP and AP patients were to PPSF (SC: −163 vs −1.40), f_{up} (SC: −163 vs −1.40), and log P (SC: −1.09 vs −1.01) for C_{trough} at steady state. Also of note was that PPSF and f_{up} are the two significantly different parameters in healthy humans and CP and AP patients. It indicates that it is more appropriate to use different PPSF and f_{up} values in the PBPK model for healthy humans and patients at different disease statuses. Since log P is an intrinsic physical and chemical parameter of IMA and not optimized, this parameter is subsequently not studied.

Next, we simulated the influence of f_{up} within the range of 0.02−0.10 and PPSF within the range of 0.5−3.0 on the C_{trough}. Figure 3C,D depicts the influence of f_{up} and PPSF on the C_{trough} in CP (400 mg OD consecutive 14 days) and AP (600 mg OD consecutive 14 days) patients, respectively. The simulations displayed that f_{up} and PPSF have a significant impact on the C_{trough} of IMA. The C_{trough} gradually descends with f_{up} and PPSF increasing and some data points are outside the efficacy and safety thresholds. The influencing trend f_{up} on the C_{trough} in CP and AP patients is quite similar, while PPSF has a wider impact on the C_{trough} in AP than those in CP patients (Figure 3D). Besides, the SD values in CP patients are significantly lower than those in AP patients. Because of the difference in f_{up} and AGP level between patients, this could in part account for the wide interpatient variation in the observed C_{trough} of IMA in the clinic.

3.3. Model Applications. *3.3.1. C_{trough} Prediction in CP and AP Patients.* The arithmetic mean values and SD values of the IMA C_{trough} were predicted by the PBPK model in CP and AP patients, respectively, under eight different doses. As seen in Table 2 and Figure 4A, except for two ratios, the other ratios were between 0.70 and 1.30. The simulations further showed that the developed PBPK model can predict accurate IMA C_{trough} at steady state. The box plot (Figure 4B) indicates that the C_{trough} values are within the desired threshold range at the doses of 400 and 600 mg in CP patients and only 600 mg in AP patients, which may ensure clinical efficacy (C_{trough} > 1000 ng/mL) and safety (C_{trough} < 3010 ng/mL). The recommendations of the dose of 400 and 600 mg in CP patients and 600 mg in AP patients by the PBPK are in good agreement with the clinical dose suggestion.[2]

3.3.2. C_{trough} Prediction in CP Patients under DDI. The predicted and observed PK data of six modulators of metabolizing enzymes and transporters have been given in supplementary Figure S2 and Table S3. The predicted PK profile of IMA when co-administered with ketoconazole is shown in Supporting Figure S3. Although our DDI simulation slightly overestimated the observed data, the 90% prediction interval almost covered the clinically observed data.[19] The predicted ratios of PK parameters are listed in Supporting Table S4. The C_{max}, C_{192}, and T_{max} ratios of IMA at 200 mg

https://doi.org/10.1021/acsomega.2c07967
ACS Omega 2023, 8, 13741−13753

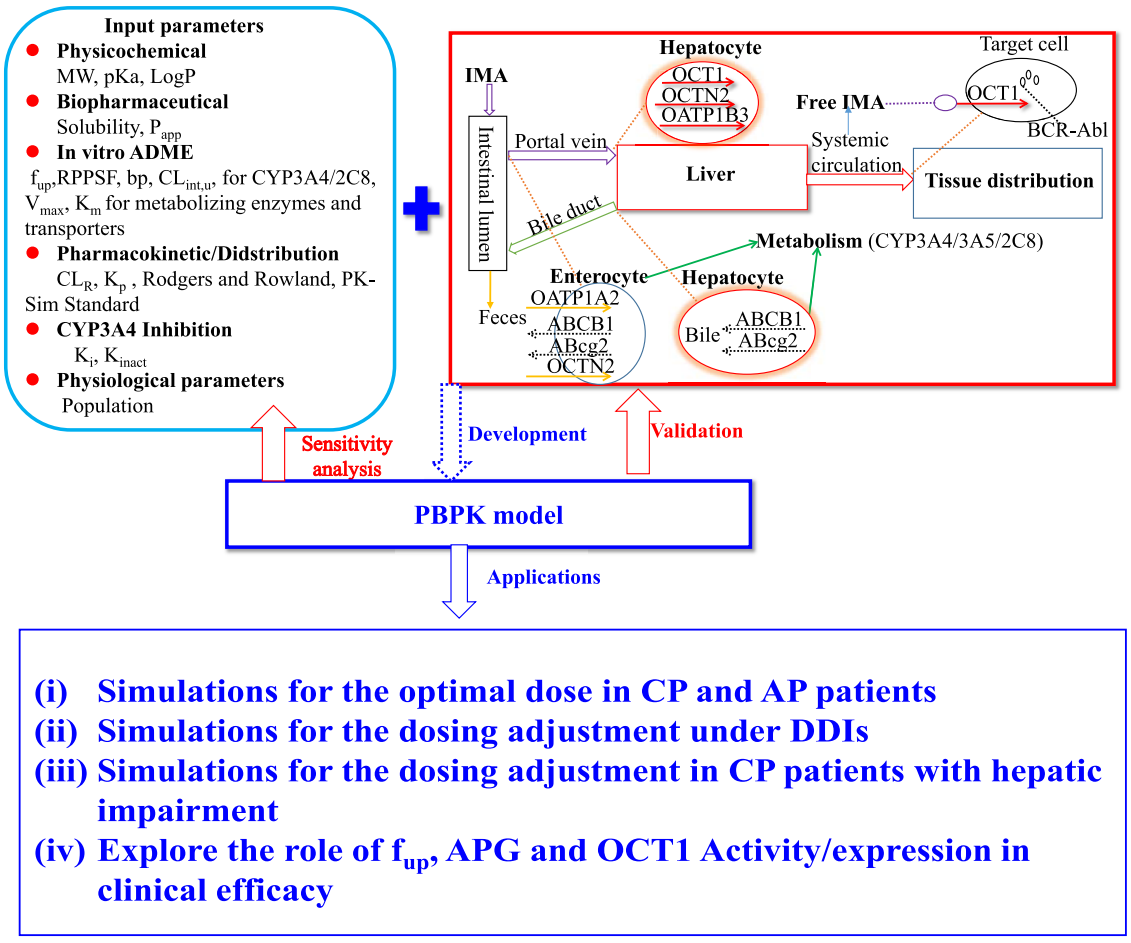

Figure 1. Generic workflow of the PBPK model.

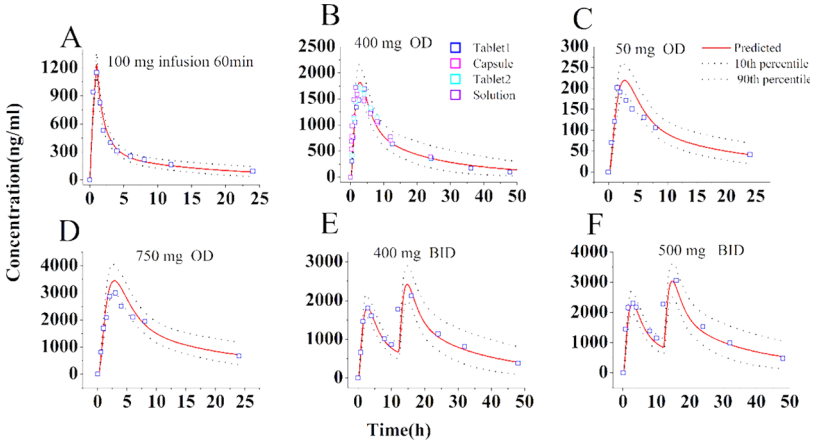

Figure 2. Simulations of the pharmacokinetics of IMA in healthy humans (A, B) and CP patients (C−F) after an oral administration. Square is the clinically observed data.

OD co-administered with ketoconazole were 1.60-, 1.96-, and 1.59-fold higher, respectively, compared with IMA only. The simulation was consistent with the clinical data,[54,55] which further confirmed the predictive power of this PBPK model.

As shown in Figure 5 and Table 4, based on the efficacy and safety thresholds, when co-administered with ketoconazole, montelukast, or verapamil, the PBPK simulations showed that 400 mg OD for IMA still represents a suitable dosing regimen in CP patients. When co-administered with itraconazole, rifampicin, or efavirenz, the simulations suggested that the dosing regimens of IMA may be modified to 300 mg OD, 400 mg BID, and 800 mg OD (or 300 mg BID), respectively. However, given the patient compliance (lowering the frequency of administration) and long-term administration safety (resulting in the teratogenic toxicity of over daily 800 mg), avoiding concomitant use with CYP3A4 reducers may be a better option for IMA clinical use. The model-based recommendations for concomitant use with ketoconazole and rifampicin are in good agreement with the clinical recommendations in DDIs.[2]

https://doi.org/10.1021/acsomega.2c07967
ACS Omega 2023, 8, 13741−13753

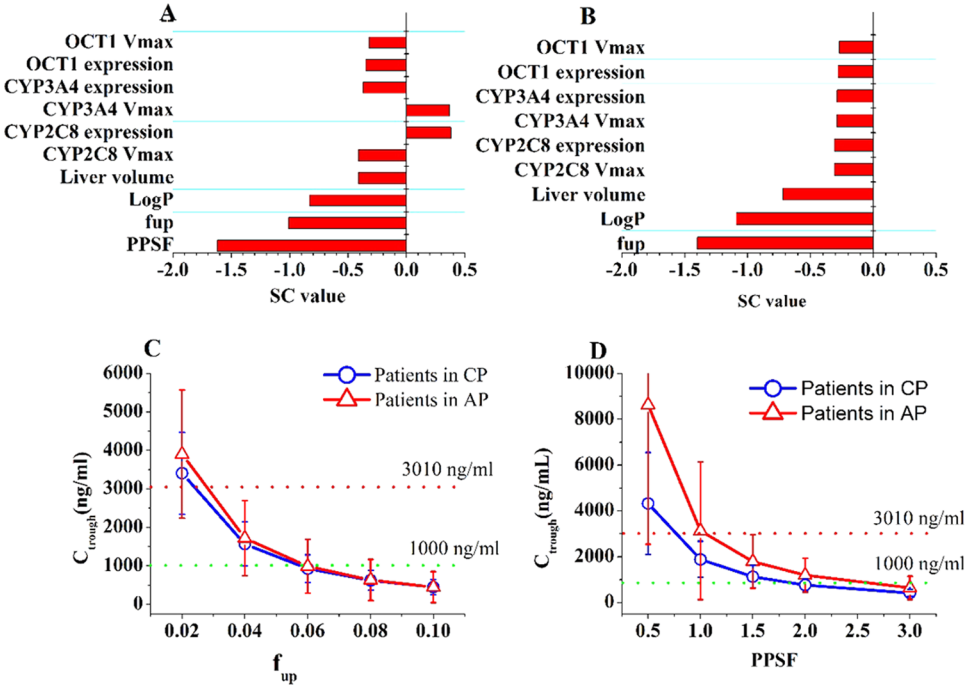

Figure 3. Sensitivity analysis of the PBPK model for CP (A) and AP (B) patients and the effect of f_{up} (C) and PPSF (D) on the C_{trough} of IMA. Data were shown as arithmetic mean values ± SD (C, D).

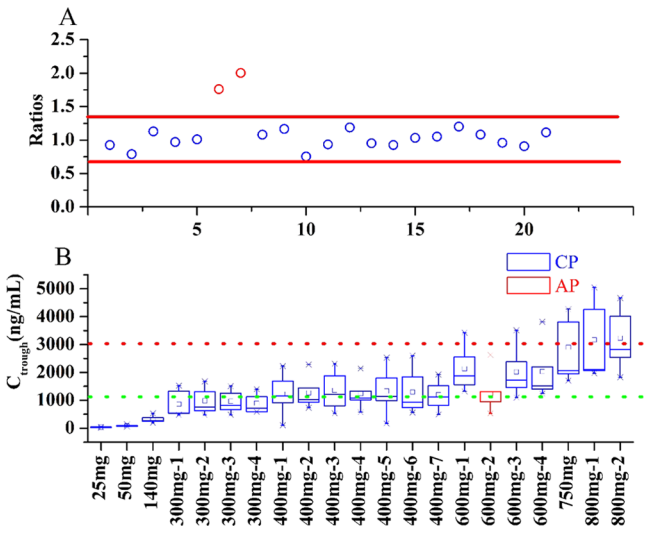

Figure 4. Ratios between predicted and observed C_{trough} (A) and box plot of predicted C_{trough} (B). Data were taken from Table 2 and shown as arithmetic mean values ± SD (B). The blue (□) and red box (□) represent data in CP and AP patients, respectively (B).

3.3.3. C_{trough} Prediction in CP Patients with Liver Dysfunction. Supporting Figure S4 shows the predicted and observed PK profiles in CP patients with hepatic impairment. The ratios between predicted and observed PK parameters are summarized in Supporting Table S5. The simulations showed that the predicted PK data were in agreement with the observed values.[52] This indicates the developed PBPK model can basically be used to predict C_{trough} in CP patients with liver impairment.

As shown in Figure 5B and Table 4, the PBPK model suggests that it is not necessary to adjust the dosing regimen for CP patients with mild and moderate hepatic impairment, which is in good agreement with the clinical recommendation.[2,52] The simulations suggested that the dosage regime in CP patients with severe hepatic impairment should be modified to 300 mg OD, which is also in good agreement with the clinical recommendation.[2]

3.3.4. Intracellular C_{trough} Prediction. It has been confirmed that the influx transporter OCT1 plays a marked role in clinical efficacy. The CML patients with low activity and expression of OCT1 could achieve a better molecular response only at a higher IMA dose (even at 800 mg OD) than the standard dose (i.e., 400 mg OD). However, the IMA plasma C_{trough} failed to reflect this influence of activity and expression of OCT1 on clinical efficacy (Figure 6A,B) because lower activity and expression of OCT1 caused a higher plasma C_{trough}. This is just in contradiction with the clinically observed result.[11] Therefore, the intracellular unbound C_{trough} and intracellular bioavailability (AUC) of IMA were simulated to assess this influence. As shown in Figure 6C,D, the activity and expression of OCT1 had a significant effect on the intracellular C_{trough} and AUC. The OCT V_{max} had slightly bigger ratios between maximal and minimal intracellular C_{trough} and between maximal and minimal intracellular AUC, compared to the OCT1 expression (C_{trough} ratio: 6.4 vs 5.0; AUC ratio: 4.6 vs 4.2). Figure 6E depicts the relationship of dose and IMA intracellular C_{trough} ratios, with a ratio of about 3-fold at 800 mg than 400 mg. When the OCT1 V_{max} and expression decreased to one-third of normal value, both intracellular C_{trough} values of IMA also decreased by approximately 3-fold (Figure 6F). The simulations indicated that the intracellular C_{trough} (or AUC) of IMA, instead of plasma C_{trough}, may guide dose adjustment to improve clinical response when patients with low OCT1 V_{max} and expression are taking IMA.

4. DISCUSSION

In this study, the PBPK model of IMA was developed successfully to simulate the C_{trough} in CP and AP patients administered alone or co-administered with other modulators

https://doi.org/10.1021/acsomega.2c07967
ACS Omega 2023, 8, 13741−13753

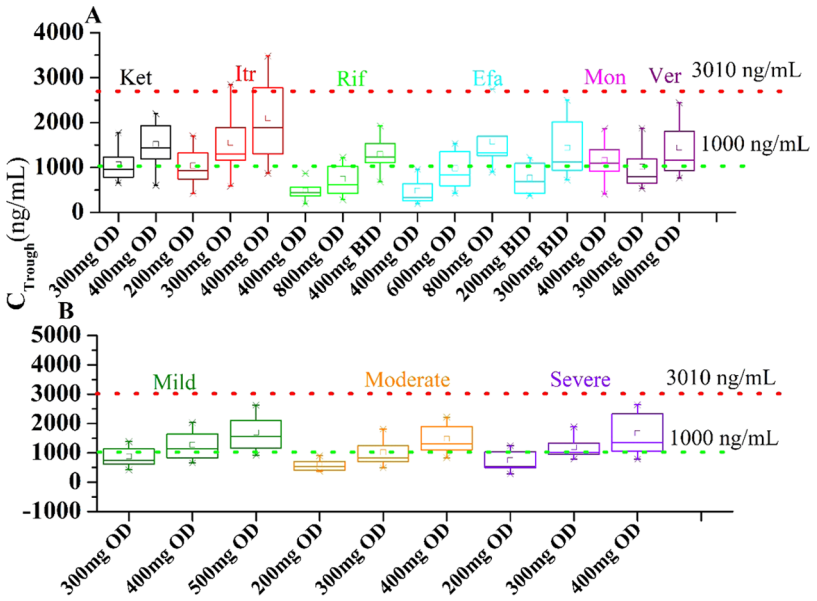

Figure 5. Box plot of predicted C_{trough} (A) in CP patients under DDIs and in CP patients with hepatic impairment (B). Data were shown as arithmetic mean values ± SD. Ket: ketoconazole, Itr: itraconazole, Rif: rifampicin, Efa: efavirenz, Mon: montelukast, and Ver: verapamil.

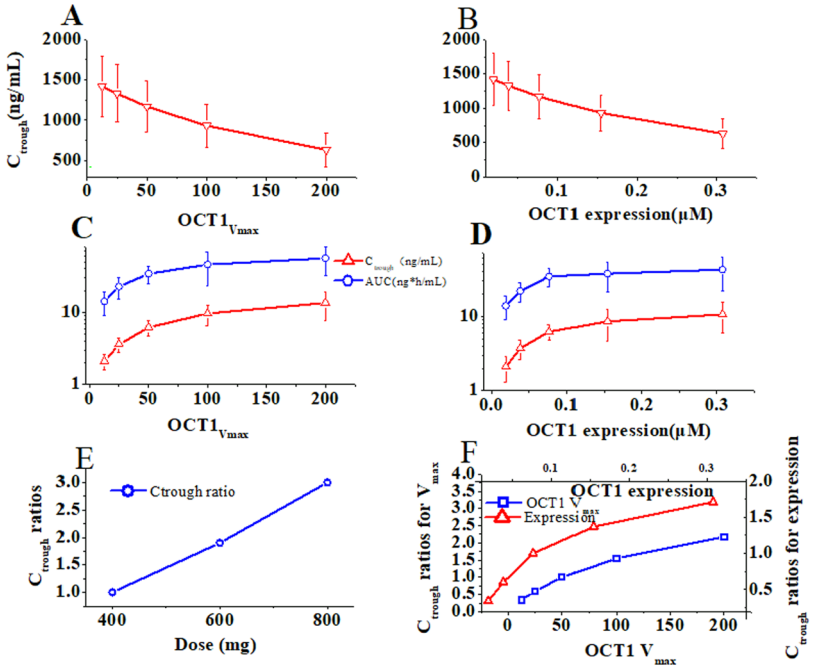

Figure 6. Influence of OCT1 V_{max} and expression on IMA PK. Influence of OCT1 V_{max} (A) and OCT1 expression (B) on the plasma C_{trough}. Influence of OCT1 V_{max} (C) and OCT1 expression (D) on C_{trough} and AUC of intracellular free IMA. The relationship between IMA dose and intracellular C_{trough} ratios (E). The plot of OCT1 V_{max} (bottom X + left Y) and OCT1 expression (top X + right Y) as a function of intracellular C_{trough} ratios (F). The Y-axis is shown in log 10 scale (C, D).

of CYP3A4/2C8 enzymes and influx transporters. Besides, the PBPK model was also used to predict the C_{trough} in CP patients with hepatic impairment. Furthermore, the optimal dosing regimens suggested by the PBPK model were provided to maximize the clinical efficacy and minimize the side effects.

4.1. Key Modeling Parameters for Healthy Humans and CP and AP Patients in the Development of the PBPK Model. Despite the fact that several PBPK models of IMA have been published,[26−29] to our knowledge, this is the first study to develop a PBPK model in healthy humans, CP patients, and AP patients by incorporating the three key modeling parameters (f_{up}, AGP level, and OCT1). The three modeling parameters differed significantly in healthy humans,[7,24,25] CP and AP patients, as well as having a marked impact on the clinical molecular response.[6,11,18] Therefore, different values of the three modeling parameters at different populations were loaded into the PBPK model to predict the C_{trough} of IMA for healthy humans and CP and AP patients, respectively. Moreover, in an *in vitro* experiment,[39] IMA was shown to be a potent mechanism-based inhibitor of CYP3A4, and in an *in vivo* study,[4] it was found to significantly increase plasma exposure of simvastatin 40 mg by about 4-fold.

https://doi.org/10.1021/acsomega.2c07967
ACS Omega 2023, 8, 13741−13753

However, in the published PBPK models of IMA, this parameter was not considered yet. Although our sensitivity analysis did not show sensitivity of the K_i CYP3A4 to C_{trough} (SC:-0.16), there was a difference of approximately 2-fold in the C_{trough} value with and without the K_i CYP3A4 in the population simulation. As a result, it is also necessary to add this parameter to the PBPK model.

4.2. Key Factors Influencing the Plasma C_{trough} of IMA in Patients. Many factors (age, gender, genetic polymorphism, DDI, gastrectomy, etc.) that could affect C_{trough} of IMA in patients have been summarized in the paper.[53] Of these factors, the IMA C_{trough} is significantly associated with the two key factors (AGP concentration[18] and DDI with CYP3A4/2C8 inducers[53]), and molecular response is significantly associated with OCT1 activity and expression[11] in the clinical setting. The sensitivity analysis in this study confirmed that the C_{trough} of IMA reduced gradually as f_{up} and AGP concentration increased (see Figure 3C,D). The previous study also demonstrated that a higher dose of IMA was required to reach comparable inhibition with *in vivo* AGP in the plasma increasing.[54] Additionally, the AGP concentration in patients at different stages differs largely, especially in AP patients.[25] In a clinical study, it was found that the AGP level was as high as about 2.3-fold in Europeans[25] and 2.5-fold in Chinese[55] compared with the control group. This could be one of the primary causes of clinically wide C_{trough} variation.

Despite the fact that IMA undergoes a minor metabolism (above 90% oral bioavailability[2]) by CYP3A4/2C8, a significant change in the C_{trough} can occur when co-administered with CYP3A4/2C8 inducers. In this study, it has been demonstrated that C_{trough} of IMA is much lower than the efficacy threshold upon concomitant use with rifampicin or efavirenz. Moreover, when co-administered with a strong CYP3A4 inhibitor (such as itraconazole), IMA C_{trough} was also significantly increased (see Figure 5A and Table 4).

Low expression and activity of OCT1 have been confirmed to be associated with suboptimal therapy.[11] The further study discovered that patients with how expression and activity of OCT1 had markedly lower intracellular IMA concentration.[56] In the clinic, patients with high OCT1 activity had a better molecular response, while patients with low OCT1 expression and activity needed higher IMA doses to overcome suboptimal response.[11] This is also the first study to examine the influence of OCT1 activity and expression on intracellular unbound IMA C_{trough} and then correlate with the oral dose (see Figure 6E). The PBPK model has also confirmed that plasma C_{trough} is not suitable as a surrogate marker of clinical efficacy for CP patients with low OCT1 activity or expression because of the contradiction of both sides (see Figure 6A,B). However, the intracellular C_{trough} of IMA can be a suitable surrogate marker of clinical efficacy because of the consistency between intracellular C_{trough} of IMA and OCT1 activity/expression (see Figure 6D). As a result, OCT1 activity and expression can be used to guide clinical dosing adjustments and may be one of the primary causes of clinical IMA resistance.[57]

4.3. Prediction Accuracy of OCT1 Uptake by the PBPK Model. When intracellular unbound drug concentration is a determinant of transporter uptake, it is difficult to provide an accurate prediction because the intracellular unbound concentration cannot be verified using the observed data. OCT1 is primarily expressed across the basolateral membrane of the hepatocyte,[58] where plasma free drug concentration drives IMA uptake. Therefore, this may enhance the prediction accuracy of the PBPK model. Based on the Michaelis−Menten kinetics, the uptake efficiency of IMA is significantly affected by IMA free plasma concentration, OCT1 V_{max}, and expression. As a result, when OCT1 V_{max} and expression are reduced, intracellular unbound IMA also significantly reduced. It was also proven by the PBPK model (see Figure 6C,D).

4.4. Recommendation of Dosing Adjustment by the PBPK Model. Based on the efficacy and safety threshold of IMA, the PBPK model suggested that 400 or 600 mg OD in CP patients and 600 mg, even a higher dose, in AP patients could represent an optimal dosing regimen (see Figure 4B and Table 2). When co-administered with rifampicin or efavirenz, the PBPK model suggested that dosing regimens of IMA may be adjusted to 400 mg BID or 800 mg OD (or 300 mg BID). However, given the safety of long-term administration (resulting in the teratogenic toxicity of over daily 800 mg), it is not suggested to co-administer with rifampicin (see Figure 5A and Table 4). This is also the first study that explores the dosing adjustment of IMA in CP patients with liver dysfunction. When co-administered with itraconazole, 300 mg BID for IMA could represent a suitable dosing regimen (see Figure 5A and Table 4). The PBPK model found that the simulated C_{trough} values in CP patients with mild and moderate differed slightly from those in CP patients with normal liver function. As a result, dosage adjustments are not required for mild and moderate hepatic impairment. In CP patients with severe hepatic impairment, the PBPK model suggested 300 mg OD as a suitable dosing regimen.

Additionally, we have also recognized that the PBPK model still has several limitations. The main limitations are (i) that active metabolite *N*-desmethyl IMA is not incorporated into this model due to a lack of modeling parameters and (ii) that only one C_{trough} data in AP patients is reported in the paper,[13] and the lack of additional C_{trough} data validates the predictive power of the PBPK model in AP patients.

5. CONCLUSIONS

Taken together, the PBPK model has been successfully developed and can accurately predict the C_{trough} in various clinical situations. In addition, this PBPK model can provide a dosage adjustment strategy for multiple IMA clinical uses.

■ ASSOCIATED CONTENT

Supporting Information

The Supporting Information is available free of charge at https://pubs.acs.org/doi/10.1021/acsomega.2c07967.

Inputting parameters used for the PBPK models of modulators in DDI simulations (Table S1); physiological parameters used in patients with liver dysfunction in the PBPK model (Table S2); mean observed and predicted PK data for the modulators of metabolizing enzymes and transporters according to their respective PBPK model (Table S3); mean observed and predicted PK data of IMA when co-administered with ketoconazole (Table S4); mean observed and predicted PK data in CP patients with hepatic impairment according to the PBPK model (Table S5); goodness-of-fit plot of the PBPK mode of IMA for predicted and observed AUC (A), C_{max} (B), and C_{end} (C) (Figure S1); mean predicted and observed plasma concentration−time profiles of ketoconazole (A), itraconazole (B), rifampicin (C), efavirenz (D), montelukast (E), and verapamil (F)

https://doi.org/10.1021/acsomega.2c07967
ACS Omega 2023, 8, 13741−13753

in healthy humans (Figure S2); predicted IMA PK profiles at 200 mg for consecutive 7 days when co-administered with 400 mg OD ketoconazole (Figure S3); and predicted and observed IMA PK profiles in CP patients with mild, moderate, and severe hepatic impairment at multiple doses (Figure S4) (PDF)

AUTHOR INFORMATION

Corresponding Authors

JinHua Wu − *Sichuan Cancer Hospital & Institute, Sichuan Cancer Center, School of Medicine, University of Electronic Science and Technology of China, Chengdu 610041, China;* orcid.org/0000-0003-0186-9624; Phone: +86 15928616219; Email: 867383422@qq.com

Xiaoang Zhao − *Institute of Chinese Material Medica China Academy of Chinese Medical Sciences, Beijing 100700, China*; Phone: +86 13811372687; Email: xazhao@icmm.ac.cn

Authors

Dongmei Gao − *Department of Medical Oncology, Bethune International Peace Hospital, Shijiazhuang 050082, China*

Guopeng Wang − *Zhongcai Health (Beijing) Biological Technology Development Co., Ltd., Beijing 101500, China*

Honghai Wu − *Department of Clinical Pharmacy, Bethune International Peace Hospital, Shijiazhuang 050082, China*

Complete contact information is available at: https://pubs.acs.org/10.1021/acsomega.2c07967

Author Contributions

#G.W. contributed equally to this work.

Funding

This study was funded by the China Academy of Chinese Medical Sciences (No. CI202A04313).

Notes

The authors declare no competing financial interest.

ACKNOWLEDGMENTS

The authors thank all those who worked so hard for their manuscript.

REFERENCES

(1) Capdeville, R.; Buchdunger, E.; Zimmermann, J.; Matter, A. Glivec (STI571, imatinib), a rationally developed, targeted anticancer drug. *Nat. Rev. Drug Discovery* **2002**, *1*, 493−502.

(2) National Institutes of Health (NIH). https://dailymed.nlm.nih.gov/dailymed/getFile.cfm?setid=7b7cc194-29e4-4484-a364-a1ac7d7d6cf5.

(3) Nebot, N.; Crettol, S.; d'Esposito, F.; Tattam, B.; Hibbs, D. E.; Murray, M. Participation of CYP2C8 and CYP3A4 in the N-demethylation of imatinib in human hepatic microsomes. *Br. J. Pharmacol.* **2010**, *161*, 1059−1069.

(4) Food and Drug Administration (FDA). https://www.accessdata.fda.gov/drugsatfda_docs/nda/2001/21-335_Gleevec_biopharmr_P1.pdf.

(5) Gschwind, H. P.; Pfaar, U.; Waldmeier, F.; Zollinger, M.; Sayer, C.; Zbinden, P.; Hayes, M.; Pokorny, R.; Seiberling, M.; Ben-Am, M.; Peng, B.; Gross, G. Metabolism and disposition of imatinib mesylate in healthy volunteers. *Drug Metab. Dispos.* **2005**, *33*, 1503−1512.

(6) Schran, H.; Peng, B.; Lloyd, P. Clinical Pharmacokinetics of Imatinib. *Clin. Pharmacokinet.* **2005**, *44*, 879−894.

(7) Harrach, S.; Barz, V.; Pap, T.; Pavenstadt, H.; Schlatter, E.; Edemir, B.; Distler, J.; Ciarimboli, G.; Bertrand, J. Notch Signaling Activity Determines Uptake and Biological Effect of Imatinib in Systemic Sclerosis Dermal Fibroblasts. *J. Invest. Dermatol.* **2019**, *139*, 439−447.

(8) Hamada, A.; Miyano, H.; Watanabe, H.; Saito, H. Interaction of imatinib mesilate with human P-glycoprotein. *J. Pharmacol. Exp. Ther.* **2003**, *307*, 824−828.

(9) Hu, S.; Franke, R. M.; Filipski, K. K.; Hu, C.; Orwick, S. J.; de Bruijn, E. A.; Burger, H.; Baker, S. D.; Sparreboom, A. Interaction of imatinib with human organic ion carriers. *Clin. Cancer Res.* **2008**, *14*, 3141−3148.

(10) Breedveld, P.; Pluim, D.; Cipriani, G.; Wielinga, P.; van Tellingen, O.; Schinkel, A. H.; Schellens, J. H. The effect of Bcrp1 (Abcg2) on the in vivo pharmacokinetics and brain penetration of imatinib mesylate (Gleevec): implications for the use of breast cancer resistance protein and P-glycoprotein inhibitors to enable the brain penetration of imatinib in patients. *Cancer Res.* **2005**, *65*, 2577−2582.

(11) White, D. L.; Giuseppe, S.; Thea, K.; Jerald, R.; Giovanni, M.; Fabrizio, P.; Dong-Wook, K.; Mark, T.; Peter, L.; Fabrizio, Q.; Simona, S.; Laura, E.; Amity, F.; Phuong, D.; Verity A, S.; Deborah, L. W. CML Patients with Low OCT-1 Activity Achieve Better Molecular Responses on High Dose Imatinib Than on Standard Dose. Those with High OCT-1 Activity Have Excellent Responses on Either Dose: A TOPS Correlative Study. *Blood* **2008**, *112*, No. 3187.

(12) Picard, S.; Titier, K.; Etienne, G.; Teilhet, E.; Ducint, D.; Bernard, M. A.; Lassalle, R.; Marit, G.; Reiffers, J.; Begaud, B.; Moore, N.; Molimard, M.; Mahon, F. X. Trough imatinib plasma levels are associated with both cytogenetic and molecular responses to standard-dose imatinib in chronic myeloid leukemia. *Blood* **2007**, *109*, 3496−3499.

(13) Forrest, D. L.; Trainor, S.; Brinkman, R. R.; Barnett, M. J.; Hogge, D. E.; Nevill, T. J.; Shepherd, J. D.; Nantel, S. H.; Toze, C. L.; Sutherland, H. J.; Song, K. W.; Lavoie, J. C.; Power, M. M.; Abou-Mourad, Y.; Smith, C. A. Cytogenetic and molecular responses to standard-dose imatinib in chronic myeloid leukemia are correlated with Sokal risk scores and duration of therapy but not trough imatinib plasma levels. *Leuk Res.* **2009**, *33*, 271−275.

(14) Van Obbergh, F.; Knoops, L.; Devos, T.; Beguin, Y.; Graux, C.; Benghiat, F.; Kargar-Samani, K.; Bauwens, D.; Efira, A.; Dubois, C.; Springael, C.; Montfort, L.; Connerotte, T.; Capron, A.; Delannoy, A.; Wallemacq, P. The clinical relevance of imatinib plasma trough concentrations in chronic myeloid leukemia. A Belgian study. *Clin. Biochem.* **2017**, *50*, 452−454.

(15) Guilhot, F.; Hughes, T. P.; Cortes, J.; Druker, B. J.; Baccarani, M.; Gathmann, I.; Hayes, M.; Granvil, C.; Wang, Y. Plasma exposure of imatinib and its correlation with clinical response in the Tyrosine Kinase Inhibitor Optimization and Selectivity Trial. *Haematologica* **2012**, *97*, 731−738.

(16) Soverini, S.; Martinelli, G.; Iacobucci, I.; Baccarani, M. Imatinib mesylate for the treatment of chronic myeloid leukemia. *Expert Rev. Anticancer Ther.* **2008**, *8*, 853−864.

(17) Rolen, K.; Shah, K. B.; Bhandari, A. Management of Chronic Myelogenous Leukemia in Pregnancy. *Anticancer Res.* **2015**, *35*, 1−12.

(18) Yoo, C.; Ryu, M. H.; Kang, B. W.; Yoon, S. K.; Ryoo, B. Y.; Chang, H. M.; Lee, J. L.; Beck, M. Y.; Kim, T. W.; Kang, Y. K. Cross-sectional study of imatinib plasma trough levels in patients with advanced gastrointestinal stromal tumors: impact of gastrointestinal resection on exposure to imatinib. *J. Clin. Oncol.* **2010**, *28*, 1554−1559.

(19) Dutreix, C.; Peng, B.; Mehring, G.; Hayes, M.; Capdeville, R.; Pokorny, R.; Seiberling, M. Pharmacokinetic interaction between ketoconazole and imatinib mesylate (Glivec) in healthy subjects. *Cancer Chemother. Pharmacol.* **2004**, *54*, 290−294.

(20) Bolton, A. E.; Peng, B.; Hubert, M.; Krebs-Brown, A.; Capdeville, R.; Keller, U.; Seiberling, M. Effect of rifampicin on the pharmacokinetics of imatinib mesylate (Gleevec, STI571) in healthy subjects. *Cancer Chemother. Pharmacol.* **2004**, *53*, 102−106.

(21) Bhattacharya, S. Double w/o/w self-nano emulsifying drug delivery system of imatinib mesylate for colon cancer treatment. *J. Mol. Liq.* **2021**, *341*, No. 117368.

(22) Farag, S.; Verheijen, R. B.; Martijn Kerst, J.; Cats, A.; Huitema, A. D.; Steeghs, N. Imatinib Pharmacokinetics in a Large Observational Cohort of Gastrointestinal Stromal Tumour Patients. *Clin. Pharmacokinet.* **2017**, *56*, 287−292.
(23) Kong, Y.; Liu, H.; Peng, H. W.; Jang, X. H.; Zou, D. Q.; Xiao, X.; Wang, F.; Wei, X. H. Simultaneous Determination of Imatinib and N-desmethyl Imatinib in Human Plasma by Two-Dimensional Liquid Chromatography and Its Clinical Application. *Chin. J. Mod. Appl. Pharm.* **2022**, *39*, 2229−2235.
(24) Kretz, O.; Weiss, H. M.; Schumacher, M. M.; Gross, G. In vitro blood distribution and plasma protein binding of the tyrosine kinase inhibitor imatinib and its active metabolite, CGP74588, in rat, mouse, dog, monkey, healthy humans and patients with acute lymphatic leukaemia. *Br. J. Clin. Pharmacol.* **2004**, *58*, 212−216.
(25) Jørgensen, H. G.; Elliott, M. A.; Allan, E. K.; Carr, C. E.; Holyoake, T. L.; Smith, K. D. α1-Acid glycoprotein expressed in the plasma of chronic myeloid leukemia patients does not mediate significant in vitro resistance to STI571. *Blood* **2002**, *99*, 713−715.
(26) Chowdhury, M. M.; Kim, D.-H.; Ahn, J.-K. A Physiologically Based Pharmacokinetic Model for Absorption and Distribution of Imatinib in Human Body. *Bull. Korean Chem. Soc.* **2011**, *32*, 3967−3972.
(27) Adiwidjaja, J.; Boddy, A. V.; McLachlan, A. J. Physiologically-Based Pharmacokinetic Predictions of the Effect of Curcumin on Metabolism of Imatinib and Bosutinib: In Vitro and In Vivo Disconnect. *Pharm. Res.* **2020**, *37*, No. 128.
(28) Adiwidjaja, J.; Boddy, A. V.; McLachlan, A. J. Implementation of a Physiologically Based Pharmacokinetic Modeling Approach to Guide Optimal Dosing Regimens for Imatinib and Potential Drug Interactions in Paediatrics. *Front. Pharmacol.* **2020**, *10*, No. 1672.
(29) Adiwidjaja, J.; Gross, A. S.; Boddy, A. V.; McLachlan, A. J. Physiologically-based pharmacokinetic model predictions of inter-ethnic differences in imatinib pharmacokinetics and dosing regimens. *Br. J. Clin. Pharmacol.* **2022**, *88*, 1735−1750.
(30) Prasad, B.; Gaedigk, A.; Vrana, M.; Gaedigk, R.; Leeder, J. S.; Salphati, L.; Chu, X.; Xiao, G.; Hop, C.; Evers, R.; Gan, L.; Unadkat, J. D. Ontogeny of Hepatic Drug Transporters as Quantified by LC-MS/MS Proteomics. *Clin. Pharmacol. Ther.* **2016**, *100*, 362−370.
(31) Brown, R. P.; Delp, M. D.; Lindstedt, S. L.; Rhomberg, L. R.; Beliles, R. P. Physiological Parameter Values for Physiologically Based Pharmacokinetic Models. *Toxicol. Ind. Health* **1997**, *13*, 407−484.
(32) Wu, C.; Li, B.; Meng, S.; Qie, L.; Zhang, J.; Wang, G.; Ren, C. C. Prediction for optimal dosage of pazopanib under various clinical situations using physiologically based pharmacokinetic modeling. *Front. Pharmacol.* **2022**, *13*, No. 963311.
(33) Couto, N.; Al-Majdoub, Z. M.; Gibson, S.; Davies, P. J.; Achour, B.; Harwood, M. D.; Carlson, G.; Barber, J.; Rostami-Hodjegan, A.; Warhurst, G. Quantitative Proteomics of Clinically Relevant Drug-Metabolizing Enzymes and Drug Transporters and Their Intercorrelations in the Human Small Intestine. *Drug Metab. Dispos.* **2020**, *48*, 245−254.
(34) Drozdzik, M.; Busch, D.; Lapczuk, J.; Muller, J.; Ostrowski, M.; Kurzawski, M.; Oswald, S. Protein Abundance of Clinically Relevant Drug Transporters in the Human Liver and Intestine: A Comparative Analysis in Paired Tissue Specimens. *Clin. Pharmacol. Ther.* **2019**, *105*, 1204−1212.
(35) Basit, A.; Radi, Z.; Vaidya, V. S.; Karasu, M.; Prasad, B. Kidney Cortical Transporter Expression across Species Using Quantitative Proteomics. *Drug Metab Dispos.* **2019**, *47*, 802−808.
(36) Pharmaceuticals and Medical Devices Agency (PMDA). https://www.info.pmda.go.jp/go/interview/1/300242_4291011F1028_1_GLI_1F.pdf.
(37) Manley, P. W.; Stiefl, N.; Cowan-Jacob, S. W.; Kaufman, S.; Mestan, J.; Wartmann, M.; Wiesmann, M.; Woodman, R.; Gallagher, N. Structural resemblances and comparisons of the relative pharmacological properties of imatinib and nilotinib. *Bioorg. Med. Chem.* **2010**, *18*, 6977−6986.
(38) Wu, C.; Liu, H.; Yu, S.; Ren, C.; Zhang, J.; Wang, G.; Li, B.; Liu, Y. Prediction of pharmacokinetics and pharmacodynamics of trelagliptin and omarigliptin in healthy humans and in patients with renal impairment using physiologically based pharmacokinetic combined DPP-4 occupancy modeling. *Biomed. Pharmacother.* **2022**, *153*, No. 113509.
(39) Filppula, A. M.; Laitila, J.; Neuvonen, P. J.; Backman, J. T. Potent mechanism-based inhibition of CYP3A4 by imatinib explains its liability to interact with CYP3A4 substrates. *Br. J. Pharmacol.* **2012**, *165*, 2787−2798.
(40) Peng, B.; Dutreix, C.; Mehring, G.; Hayes, M. J.; Ben-Am, M.; Seiberling, M.; Pokorny, R.; Capdeville, R.; Lloyd, P. Absolute bioavailability of imatinib (Glivec) orally versus intravenous infusion. *J. Clin. Pharmacol.* **2004**, *44*, 158−162.
(41) Nikolova, Z.; Peng, B.; Hubert, M.; Sieberling, M.; Keller, U.; Ho, Y. Y.; Schran, H.; Capdeville, R. Bioequivalence, safety, and tolerability of imatinib tablets compared with capsules. *Cancer Chemother. Pharmacol.* **2004**, *53*, 433−438.
(42) Peng, B.; Hayes, M.; Resta, D.; Racine-Poon, A.; Druker, B. J.; Talpaz, M.; Sawyers, C. L.; Rosamilia, M.; Ford, J.; Lloyd, P.; Capdeville, R. Pharmacokinetics and pharmacodynamics of imatinib in a phase I trial with chronic myeloid leukemia patients. *J. Clin. Oncol.* **2004**, *22*, 935−942.
(43) Ogata, K.; Kimura, A.; Nakazawa, N.; Suzuki, M.; Yanoma, T.; Ubukata, Y.; Iwamatsu, K.; Kogure, N.; Yanai, M.; Kuwano, H. Long-Term Imatinib Treatment for Patients with Unresectable or Recurrent Gastrointestinal Stromal Tumors. *Digestion* **2018**, *97*, 20−25.
(44) IJzerman, N. S.; Groenland, S. L.; Koenen, A. M.; Kerst, M.; van der Graaf, W. T. A.; Rosing, H.; Beijnen, J. H.; Huitema, A. D. R.; Steeghs, N. Therapeutic drug monitoring of imatinib in patients with gastrointestinal stromal tumours - Results from daily clinical practice. *Eur. J. Cancer* **2020**, *136*, 140−148.
(45) Saeheng, T.; Na-Bangchang, K.; Siccardi, M.; Rajoli, R. K. R.; Karbwang, J. Physiologically-Based Pharmacokinetic Modeling for Optimal Dosage Prediction of Quinine Coadministered With Ritonavir-Boosted Lopinavir. *Clin. Pharmacol. Ther.* **2020**, *107*, 1209−1220.
(46) Li, G.; Yi, B.; Liu, J.; Jiang, X.; Pan, F.; Yang, W.; Liu, H.; Liu, Y.; Wang, G. Effect of CYP3A4 Inhibitors and Inducers on Pharmacokinetics and Pharmacodynamics of Saxagliptin and Active Metabolite M2 in Humans Using Physiological-Based Pharmacokinetic Combined DPP-4 Occupancy. *Front. Pharmacol.* **2021**, *12*, No. 746594.
(47) Food and Drug Administration (FDA). https://www.accessdata.fda.gov/drugsatfda_docs/nda/2017/210259Orig1s000MultidisciplineR.pdf.
(48) Hanke, N.; Frechen, S.; Moj, D.; Britz, H.; Eissing, T.; Wendl, T.; Lehr, T. PBPK Models for CYP3A4 and P-gp DDI Prediction: A Modeling Network of Rifampicin, Itraconazole, Clarithromycin, Midazolam, Alfentanil, and Digoxin. *CPT: Pharmacometrics Syst. Pharmacol.* **2018**, *7*, 647−659.
(49) Dixit, V.; Moore, A.; Tsao, H.; Hariparsad, N. Application of Micropatterned Cocultured Hepatocytes to Evaluate the Inductive Potential and Degradation Rate of Major Xenobiotic Metabolizing Enzymes. *Drug Metab. Dispos.* **2016**, *44*, 250−261.
(50) Walsky, R. L.; Gaman, E. A.; Obach, R. S. Examination of 209 drugs for inhibition of cytochrome P450 2C8. *J. Clin. Pharmacol.* **2005**, *45*, 68−78.
(51) Parvez, M. M.; Kaisar, N.; Shin, H. J.; Lee, Y. J.; Shin, J. G. Comprehensive Substrate Characterization of 22 Antituberculosis Drugs for Multiple Solute Carrier (SLC) Uptake Transporters In Vitro. *Antimicrob Agents Chemother.* **2018**, *62*, No. e00512-18.
(52) Ramanathan, R. K.; Egorin, M. J.; Takimoto, C. H.; Remick, S. C.; Doroshow, J. H.; LoRusso, P. A.; Mulkerin, D. L.; Grem, J. L.; Hamilton, A.; Murgo, A. J.; Potter, D. M.; Belani, C. P.; Hayes, M. J.; Peng, B.; Ivy, S. P. Phase I and pharmacokinetic study of imatinib mesylate in patients with advanced malignancies and varying degrees of liver dysfunction: a study by the National Cancer Institute Organ Dysfunction Working Group. *J. Clin. Oncol.* **2008**, *26*, 563−569.
(53) Chen, Y.; Dong, X.; Wang, Q.; Liu, Z.; Dong, X.; Shi, S.; Xiao, H. Factors Influencing the Steady-State Plasma Concentration of

https://doi.org/10.1021/acsomega.2c07967
ACS Omega 2023, 8, 13741−13753

Imatinib Mesylate in Patients With Gastrointestinal Stromal Tumors and Chronic Myeloid Leukemia. *Front. Pharmacol.* **2020**, *11*, No. 569843.
(54) Carlo, G. P.; Rossella, B.; Philipp, L. C.; Massimo, Z.; Cabrita, G.; Loredana, C.; Francesca, R.; Elisabetta, G.; Josef, B.; Robert, C.; Pietro, P.; Enrico, P.; Gianmarco, C.; Franca, F.; Maurizio, D. Role of α1 acid glycoprotein in the in vivo resistance of human bcr-abl+ leukemic cells to the abl inhibitor sti571. *JNCI, J. Natl. Cancer Inst.* **2000**, *20*, 1641−1650.
(55) Zhong, J. S.; MFY; Xu, D.; Dai, M.; Wei, Y. Q.; Zhou, H. S. Relationship between serum α1-acid glycoprotein and imatinib concentration and efficacy in patients with chronic myeloid leukemia. *Nail Med. J. China* **2011**, *91*, 30.
(56) White, D. L.; Saunders, V. A.; Dang, P.; Engler, J.; Venables, A.; Zrim, S.; Zannettino, A.; Lynch, K.; Manley, P. W.; Hughes, T. Most CML patients who have a suboptimal response to imatinib have low OCT-1 activity: higher doses of imatinib may overcome the negative impact of low OCT-1 activity. *Blood* **2007**, *110*, 4064−4072.
(57) An, X.; Tiwari, A. K.; Sun, Y.; Ding, P. R.; Ashby, C. R., Jr.; Chen, Z. S. BCR-ABL tyrosine kinase inhibitors in the treatment of Philadelphia chromosome positive chronic myeloid leukemia: a review. *Leuk Res.* **2010**, *34*, 1255−1268.
(58) Koepsell, H. Update on drug-drug interaction at organic cation transporters: mechanisms, clinical impact, and proposal for advanced in vitro testing. *Expert Opin. Drug Metab. Toxicol.* **2021**, *17*, 635−653.

https://doi.org/10.1021/acsomega.2c07967
ACS Omega 2023, 8, 13741−13753